

The Urban Impact of AI: Modeling Feedback Loops in Next-Venue Recommendation

Giovanni Mauro^{1,2*}, Marco Minici³ and Luca Pappalardo^{1,2}

¹ ISTI-CNR, via G. Moruzzi 1, Pisa, 56124, Italy.

² Scuola Normale Superiore, Piazza dei Cavalieri, 7, Pisa, 56126, Italy.

² ICAR-CNR, Via Pietro Bucci 8/9c, Rende, 87036, Italy.

*Corresponding author(s). E-mail(s): giovanni.mauro@sns.it;

Contributing authors: marco.minici@icar.cnr.it;

luca.pappalardo@isti.cnr.it;

Abstract

Next-venue recommender systems are increasingly embedded in location-based services, shaping individual mobility decisions in urban environments. While their predictive accuracy has been extensively studied, less attention has been paid to their systemic impact on urban dynamics. In this work, we introduce a simulation framework to model the human–AI feedback loop underpinning next-venue recommendation, capturing how algorithmic suggestions influence individual behavior, which in turn reshapes the data used to retrain the models. Our simulations, grounded in real-world mobility data, systematically explore the effects of algorithmic adoption across a range of recommendation strategies. We find that while recommender systems consistently increase individual-level diversity in visited venues, they may simultaneously amplify collective inequality by concentrating visits on a limited subset of popular places. This divergence extends to the structure of social co-location networks, revealing broader implications for urban accessibility and spatial segregation. Our framework operationalizes the feedback loop in next-venue recommendation and offers a novel lens through which to assess the societal impact of AI-assisted mobility—providing a computational tool to anticipate future risks, evaluate regulatory interventions, and inform the design of ethic algorithmic systems.

Keywords: Human-AI Feedback Loop, Next-Venue Recommendation, Diversity, Ethical Recommender Systems

1 Introduction

Recommender systems have become increasingly pervasive in urban life, seamlessly integrated into the online platforms that millions of individuals rely on to navigate cities and make everyday decisions (Pedreschi et al. 2025; Quijano-Sánchez et al. 2020). Among the most influential are next-venue recommenders, which suggest places to visit – such as restaurants, cafés, parks, shops, or cultural landmarks – through widely used location-based services like Google Maps, TripAdvisor, Yelp, and Foursquare. These platforms act as decision-making assistants, offering personalized suggestions in real time based on an individual’s current location, mobility history, preferences, and contextual factors such as time of day or weather.

The growing importance of next-venue recommenders stems from both their ubiquity and impact. As mobile devices and GPS-enabled apps become indispensable tools in daily urban routines, individuals increasingly delegate micro-decisions (where to eat, shop, or spend leisure time) to algorithmic systems. These recommendations are powered by machine learning techniques, often based on deep learning architectures, which can model complex spatiotemporal patterns of behavior and predict future movements with high accuracy (Luca et al. 2021). By shaping when and where people move in the city, next-venue recommenders exert a subtle yet powerful influence on urban flows, human movements, and the popularity of venues. For example, a recent study shows that the recommender system implemented by Uber Eats led to significant improvements in consumer engagement and gross bookings, influencing the popularity of certain restaurants (Wang et al. 2025).¹

While much research has focused on developing accurate and efficient next-venue recommendation algorithms (Luca et al. 2021; Koolwal and Mohbey 2020), and recent work has begun to question their evaluation methods and capability to generalize to unknown situations (Luca et al. 2023), their broader implications for urban dynamics remain largely unexplored (Pedreschi et al. 2025; Pappalardo et al. 2023). This gap in understanding is particularly pressing in light of recent regulatory developments. The European Union’s Digital Services Act introduces mandatory risk assessment requirements for very large online platforms and search engines, with a focus on evaluating their impact on users and society.² However, no robust framework currently exists to assess the systemic risks posed by next-venue recommenders.

Understanding the impact of these AI systems is particularly challenging because their interaction with individuals creates an intricate feedback loop (Pedreschi et al. 2025; Tsvetkova et al. 2024): each individual decision contributes to form the big data that is used to train or update the recommender system, which in turn influences future decisions about where to go. This recursive process generates a continuously evolving cycle that can reshape the urban landscape. Capturing this feedback loop in its entirety – encompassing algorithmic recommendations, user responses, the ongoing retraining of machine learning models, and the dynamic evolution of system behavior – is difficult, as it would require direct access to the platforms delivering the recommender systems. At present, only the companies operating these platforms have the technical and legal means to observe and analyze the full loop. It is therefore not

¹See also <https://www.gsb.stanford.edu/insights/better-way-make-recommendations-power-popular-platforms>

²<https://eur-lex.europa.eu/legal-content/EN/TXT/?uri=CELEX%3A32022R2065>

surprising that most research to date has focused on mathematical formalization and modeling of the feedback loop, rather than its empirical measurement (Pappalardo et al. 2024; Chen et al. 2023). While some progress has been made in this direction for other human–AI ecosystems – such as social media, online retail, and generative AI (Lesota et al. 2024; Zhou et al. 2024; Shumailov et al. 2024; Mansoury et al. 2020; Jiang et al. 2019; Sun et al. 2019; Nguyen et al. 2014) – no equivalent effort has yet been undertaken for next-venue recommender systems despite their growing influence on urban dynamics.

In this article, we model the feedback loop between individuals and next-venue recommender systems to simulate its impact on individual behaviour and the urban environment. We implement our simulation framework across multiple types of recommender systems, trained on real-world data describing all recorded venue visits by individuals in New York City. At the core of our model is the venue selection mechanism, which governs how individuals decide where to go next. With a given probability, an individual follows the suggestion of the recommender system. With the complementary probability, the individual makes an autonomous choice, which we simulate using a well-established mechanistic model of human mobility. By running the simulation over several weeks, we study how varying degrees of algorithmic influence affect the visitation diversity of individuals, the popularity of venues, and the individuals’ co-location network.

Our results reveal that the impact of recommender systems varies across the models investigated, yet a consistent pattern emerges: at the individual level, we find an increased diversification in venue visits, while at the collective level, diversity decreases reflecting a rise in inequality in venue popularity. We further examine the tension between personalization and concentration, and find that the increase in individual diversity is largely driven by visits to already popular venues. This mirrors patterns observed in other human–AI ecosystems, where recommender systems improve individual choice but simultaneously amplify system-wide popularity bias. Our study thus adds another piece to the broader mosaic of how recommender systems shape complex social systems, highlighting the structural consequences of algorithmic mediation across diverse domains.

The remainder of the paper is organized as follows. Section 2 reviews the existing literature on the impact of recommender systems on urban dynamics. Section 3 presents our simulation framework and details the modeling of the human–recommender feedback loop. Section 4 outlines the experimental setup, and Section 5 reports the results of our simulations. Section 6 interprets our findings in the broader context of human–AI coevolution. Finally, Section 7 concludes the paper by discussing the limitations of our study and proposing directions for future research.

2 Related Work

This section reviews key experimental studies that examine how recommendation systems impact urban dynamics.

A growing body of research investigates the impact of GPS-based navigation systems on the urban environment. Arora et al. (2021) simulate the effects of Google

Maps navigation in Salt Lake City, reporting average reductions of 6.5% in travel time and 1.7% in CO₂ emissions. These benefits are even more pronounced for individuals whose routes were altered by the route recommendations. [Cornacchia et al. \(2022\)](#) use TomTom APIs to simulate navigation services in Milan, showing that adoption rates critically shape system-wide outcomes: emissions increase at very low or very high adoption levels but decrease when adoption stabilizes around 50%. [Perez-Prada et al. \(2017\)](#) show that widespread adoption of eco-routing during congestion can reduce CO₂ and NO_x emissions by 10% and 13%, respectively. However, these gains come with trade-offs: NO_x exposure increases by 20%, travel times rise by 28%, and vehicle concentration in downtown areas grows by 16%. Two studies simulate routing systems in Florence, Rome, and Milan to show that prioritizing diversity in routing can lead to more balanced traffic distribution, improved road network coverage, and reductions in CO₂ emissions ([Cornacchia et al. 2024, 2023](#)).

Several studies examine how recommendation systems on house-renting platforms influence socio-economic dynamics, often reinforcing systemic inequalities. [Edelman and Luca \(2014\)](#) uncover racial disparities in New York City's Airbnb market, reporting a 12% revenue gap between Black and non-Black hosts, even after controlling for property characteristics and guest ratings. [Zhang et al. \(2021\)](#) expand on this finding, showing that Airbnb's smart-pricing algorithm can reduce these price disparities and improve revenues for Black hosts, although it does not entirely eliminate systemic bias.

Additional research investigates how ride-hailing and ride-sharing platforms influence urban mobility through algorithmic matching and incentive design. [Bokányi and Hannák \(2020\)](#) find that a ride recommender system prioritizing lower-earning drivers in New York City would reduce disparities and increase driver earnings compared to prioritizing the closest available vehicle. [Afèche et al. \(2023\)](#) analyze passenger-driver matching and centralized dispatch algorithms, showing that while centralized control improves efficiency, it can restrict service access in less densely populated areas, exacerbating spatial inequities.

Position of our work

A review of the literature reveals two major gaps ([Pappalardo et al. 2024](#)). First, there are no existing studies that have examined the actual or potential impact of next-venue recommendation systems on urban dynamics. Second, although a growing body of research outside the urban domain has begun to formalise and model human–AI feedback loops ([Sun et al. 2019; Mansoury et al. 2020; Jiang et al. 2019; Nguyen et al. 2014; Shumailov et al. 2024; Lesota et al. 2024; Zhou et al. 2024](#)), there has been little attention given to how these feedback loops manifest in urban environments or how they can be formally modelled.

A notable exception is the work by [Ensign et al. \(2018\)](#), which shows how a feedback loop can distort the allocation of police resources, reinforce existing biases, and generate unrealistic crime distributions in a city. By introducing corrective mechanisms to prevent repeated deployments in the same areas, the authors demonstrate that even minor changes in algorithmic design can significantly influence urban outcomes. While this study represents a pioneering effort, the modelling of human–AI feedback loops and their effects on urban mobility and spatial behaviour remains largely unexplored.

Our work takes a first step toward addressing these gaps by explicitly modeling the human–AI feedback loop in the context of next-venue recommendation systems. We introduce an open-source simulation framework that enables the systematic evaluation of how different recommendation algorithms influence key aspects of urban dynamics, such as venue popularity and individual visitation patterns.

3 Methodology

Our study is grounded in a simulation framework designed to model the human–AI feedback loop in the context of next-venue recommendation. In Section 3.1, we introduce the notation and formal definitions necessary to understand the simulation framework. Section 3.2 presents the simulation methodology in detail, while Section 3.3 describes the metrics used to evaluate the impact of the feedback loop on the urban complex system.

3.1 Preliminaries

Let U be a set of individuals and V a set of public venues. We define a dataset $D \subseteq U \times V \times T$ as an interaction matrix, where each tuple $(u, v, t) \in D$ represents a visit by individual $u \in U$ to venue $v \in V$ at time $t \in T$. The dataset describes all visits up to a time T_{\max} , and tuples in it are sorted chronologically. For each individual $u \in U$, we define $D_u = \{v_1, \dots, v_n\}$ as the time-ordered sequence of venues visited by u in D , sorted by timestamp. The dataset D is partitioned into two disjoint subsets: a training set D_{train} , which contains all tuples $(u, v, t) \in D$ such that $t \leq T_{\text{train}}$, and a post-training set D_{post} , which contains all tuples such that $T_{\text{train}} < t \leq T_{\max}$.

Each venue $v \in V$ is associated with a categorical label provided by a function $\ell : V \rightarrow C$, where $C = \{c_1, \dots, c_z\}$ is a predefined set of venue categories (e.g., *restaurant*, *museum*, *school*). Venues are geolocated via a function $\pi : V \rightarrow [-90, 90] \times [-180, 180]$, which maps a venue $v \in V$ to its latitude and longitude coordinates. The geographical distance between two venues $v_i, v_j \in V$ is computed as the great-circle distance between their coordinates on the Earth’s surface.

We define a scoring function $\mathcal{R}_\theta : U \times V \times T \rightarrow [0, 1]$ with parameters θ and trained on a subset $D_{\text{train}} \subset D$, which includes all visits observed up to time $T_{\text{train}} \ll T_{\max}$. For any individual $u \in U$, venue $v \in V$, and time $t \in T$, the score $\mathcal{R}_\theta(u, v, t)$ represents the estimated probability that u will visit v as following location at a future time $t' > t$. The recommender system, \mathcal{A} , is an operator that, for a given user u and time t , ranks all candidate venues according to their scores $\mathcal{R}_\theta(u, v, t)$ and returns the top- k venues from this ranking.

3.2 Simulation Framework

Given the sets U , V , the datasets D , D_{train} and D_{post} , the scoring function $\mathcal{R}_\theta(u, v, t)$ and the recommender system \mathcal{A} , our framework simulates the generation of visits to venues in V by individuals in U . In the simulation framework, an individual’s decision on which venue to visit may be influenced by the recommendations provided by \mathcal{A} , modelling a scenario in which algorithmic suggestions shape user behaviour. As the

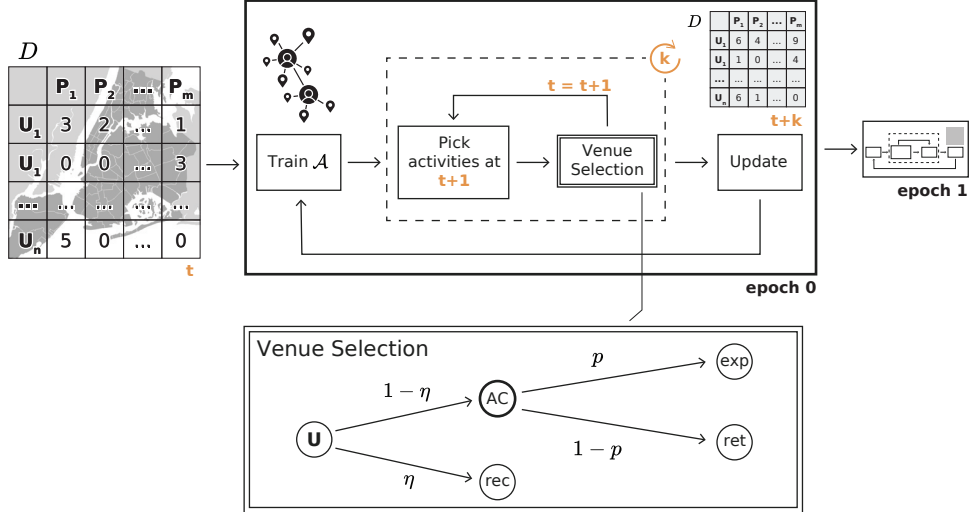


Fig. 1: Overview of the simulation framework. At each step of the simulation, an individual chooses between relying on recommendations (with probability η) or an autonomous choice (AC) (with probability $1 - \eta$). AC is further split between exploration (with probability p) and preferential return (with probability $1 - p$), where p is a fixed parameter equals to $\rho \cdot S^{-\gamma}$ where S is the number of distinct previously visited locations. Initially, a recommender system \mathcal{A} is trained on historical visit data. At each timestep $t + 1$, individuals' next venues are selected, and the dataset is updated accordingly. After k timesteps, the recommender is retrained, allowing the feedback loop between individual decisions and algorithmic suggestions to evolve over time.

simulation goes by, a dataset \mathcal{S} is generated, which contains the simulated visits of the individuals to the venues. Figure 1 provides an overview of the simulation framework, illustrating the key components and the flow of interactions between individuals and the recommender system.

The mobility simulation for each individual $u \in U$ is outlined in Algorithm 1. The process begins with training the recommender system \mathcal{A} on the training dataset D_{train} (line 1). The simulation then iterates over each visit tuple $(u, v, t) \in D_{\text{post}}$ (line 5), simulating user mobility in three sequential steps: category selection (line 6), where the category of the next venue is taken from dataset D_{post} ; venue selection (line 7), where the specific venue is selected based on the chosen category and the individual's decision to use or not the recommender system; and algorithm retraining (line 10), which updates \mathcal{A} every Δ time units to incorporate newly simulated data in \mathcal{S} .

Category selection

For each visit by u in D_{post} , we observe the actual venue $v \in V$ visited by u and determine the corresponding category $c = \ell(v)$.

Algorithm 1 Simulation Framework

Input Data: Dataset of visits D , Training dataset D_{train} , Observation dataset D_{post} .
All datasets are sorted by time.

Hyperparameters: Adoption rate η , Retraining frequency Δ

Output Data: Dataset \mathcal{S} of simulated visits

```
1:  $\mathcal{A} \leftarrow \text{AlgorithmTraining}(D_{\text{train}})$                                  $\triangleright$  Train the recommender system
2:  $(u, v, t) \leftarrow \text{last}(D_{\text{train}})$                                       $\triangleright$  Last tuple of the training dataset
3:  $t_{\text{last\_training}} \leftarrow t$                                                $\triangleright$  Timestamp of the last training
4:  $\mathcal{S} \leftarrow \emptyset$ 
5: for  $(u, v_{\text{current}}, t)$  in  $D_{\text{post}}$  do                                $\triangleright$  Iterate over the visits
6:    $c \leftarrow \text{CategorySelection}(v_{\text{current}})$            $\triangleright$  Select the category of the next venue
7:    $v_{\text{next}} \leftarrow \text{VenueSelection}(u, v_{\text{current}}, t, \mathcal{A}, \eta)$        $\triangleright$  Select the next venue
8:    $\mathcal{S} \leftarrow \mathcal{S} \cup \{(u, v_{\text{next}}, t)\}$             $\triangleright$  Add the simulated visit to the dataset
9:   if  $t - t_{\text{last\_training}} > \Delta$  then            $\triangleright$  Check if it's time to retrain the model
10:     $\mathcal{A} \leftarrow \text{AlgorithmTraining}(D_{\text{train}} \cup \mathcal{S})$       $\triangleright$  Retrain the recommender system
11:     $t_{\text{last\_training}} \leftarrow t$                             $\triangleright$  Update last training time
12:   end if
13: end for
```

Venue Selection

Given the target category c representing the type of venue to be visited, the individual $u \in U$ must select a specific venue of that category. The venue selection process is detailed in Algorithm 2.

The first step involves deciding whether to rely on the recommender system \mathcal{A} (line 4 of Algorithm 2). This decision reflects the user's choice between following algorithmic suggestions or acting autonomously. It is modelled as a Bernoulli trial with success probability $\eta \in [0, 1]$, referred to as the adoption rate, which quantifies the likelihood that u accepts the recommendation. The parameter η plays a central role in the simulation, controlling the extent to which user behavior is shaped by the recommender. If the Bernoulli trial succeeds, u follows the recommendation (recommendation-based choice, line 5); otherwise, u selects a venue independently (autonomous choice, lines 7–10).

Recommendation-based choice

If individual u follows the suggestion of the recommender system \mathcal{A} (line 5 of Algorithm 2), a set of candidate venues $V_{c,r} \subseteq V$ is retrieved (line 3, Algorithm 2). This set includes all venues belonging to the target category c and located within a radius r from the individual's current venue v_{current} .

The radius r is sampled from the empirical distribution of jump lengths observed in D , reflecting the tendency of individuals to prefer short-range displacements (Pappalardo et al. 2015; Gonzalez et al. 2008). This distribution is obtained by enumerating all consecutive venue pairs (v_{i-1}, v_i) in the visit sequences D_u for each user $u \in U$, and computing the great-circle distance between v_{i-1} and v_i using their geographic coordinates.

Algorithm 2 Venue Selection for Individual u

Input Data: Venue set V , Current venue $v_{\text{current}} \in V$, Target category c , User history D_u , Training dataset D_{train} , Simulated dataset \mathcal{S} , Jump length distribution $\mathcal{P}_{\text{jump}}$

Hyperparameters: Adoption rate η , Exploration probability p

Output Data: Selected venue v_{next}

```
1:  $r \leftarrow \text{Sample}(\mathcal{P}_{\text{jump}})$             $\triangleright$  Sample a jump length from the empirical distribution
2:  $r^* \leftarrow \text{Median}(\mathcal{P}_{\text{jump}})$            $\triangleright$  Median of jump distribution
3:  $V_{c,r} \leftarrow \{v \in V \mid \ell(v) = c \wedge \text{dist}(v_{\text{current}}, v) \leq r\}$            $\triangleright$  Candidate venues
4: if  $\text{Bernoulli}(\eta)$  then
5:    $v_{\text{next}} \leftarrow \mathcal{A}(u, V_{c,r})$            $\triangleright$  Select venue using recommender system
6: else
7:   if  $\text{Bernoulli}(1 - p)$  then           $\triangleright$  Return to a previously visited venue
8:      $v_{\text{next}} \leftarrow \text{PreferentialReturn}(D_u, c)$ 
9:   else           $\triangleright$  Explore a new venue
10:     $v_{\text{next}} \leftarrow \text{Explore}(V_{c,r}, D_u, r^*)$ 
11:   end if
12: end if
```

Each venue $v \in V_{c,r}$ is assigned a score $\mathcal{R}_\theta(u, v, t)$, and the resulting set of scores S is normalized via min-max normalization to produce the set of normalized scores \hat{S} . The recommender system \mathcal{A} then returns the top- k venues in $L \in V_{c,r}$ based on \hat{S} . Finally, u selects a venue $v_{\text{next}} \in L$ with probability proportional to its normalized score $\hat{S}(v)$.

Autonomous choice

If the individual u moves independently of the recommender system \mathcal{A} (line 7 of Algorithm 2), we model their venue choice using a modified version of the Exploration and Preferential Return (EPR) model, a well-established framework for human mobility introduced by [Song et al. \(2010\)](#). The EPR model captures the fundamental mechanism of human mobility as a trade-off between returning to previously visited locations and exploring new ones. At each decision point, the individual u chooses between:

- **Preferential return** (line 8, Algorithm 2): with probability $1 - p$, the individual selects a venue from their set of previously visited locations, with probability proportional to the number of times each venue has been visited by u .
- **Exploration** (line 10, Algorithm 2): with probability p , the individual selects a new (unvisited) venue located within a radius r , where r is sampled from the empirical distribution of jump lengths observed in D . Among the venues within this radius, the probability of selecting a specific venue v is proportional to its relevance.

The relevance of a venue $v \in V$ is defined as the number of other venues located within a fixed radius r^* from v , where r^* is set to the median of the jump length distribution computed on D . Intuitively, a venue is more relevant if it lies in a dense area where many other venues fall within this typical range, making it more likely to

be part of users' mobility patterns. Formally, the relevance is given by $rel(v) = |\{v' \in V \setminus \{v\} | d(v, v') \leq r^*\}|$.

In cases where a user does not have enough venues of the target category within the sampled radius or in other edge scenarios, a fallback mechanism is activated to ensure a valid venue is selected. Further details are provided in Appendix A.

Algorithm retraining

The recommender system \mathcal{A} is periodically retrained during the simulation at fixed intervals of Δ time units (line 10, Algorithm 1). At each retraining step, the model is updated using an enriched dataset consisting of the original training set D_{train} combined with the set \mathcal{S} of simulated visits generated up to that point, i.e., $D_{\text{train}} \cup \mathcal{S}$. In practice, this step corresponds to updating the parameters θ of the scoring function \mathcal{R}_θ based on this augmented dataset.

This retraining procedure allows \mathcal{A} to iteratively refine its understanding of individual preferences by incorporating both historical and simulated behavioral data. In doing so, it captures the dynamic nature of the human–AI feedback loop, where algorithmic outputs influence human behavior, which in turn shapes future recommendations.

3.3 Metrics

We assess the impact of the human–AI feedback loop on urban dynamics from two complementary perspectives: one focused on venues and the other on individuals.

Venue perspective

We evaluate the inequality in the distribution of visits across venues using the Gini index. This measure captures the extent to which visits are concentrated on a subset of venues: a Gini index of 0 indicates perfect equality (all venues receive the same number of visits), while higher values indicate increasing concentration of visits on fewer venues. Our use of the Gini index is motivated by findings in the literature showing that recommender systems can amplify inequality in the distribution of consumed items (Pedreschi et al. 2025; Pappalardo et al. 2024; Boratto et al. 2021; Elahi et al. 2021; Lee and Hosanagar 2019). In our context, this dynamic reflects how algorithmic recommendations may disproportionately direct individuals toward a limited number of venues, increasing their popularity while marginalizing others.

Given a dataset of visits D , we compute the collective Gini index as:

$$G = \frac{1}{|V|} \left(|V| + 1 - 2 \cdot \frac{\sum_{i=1}^{|V|} (|V| + 1 - i)x_i}{\sum_{v \in V} x_i} \right), \quad (1)$$

where $x_i = |(u, v, t) \in D : v = v_i|$ is the total number of visits to venue $v_i \in V$, and the values x_i are sorted in ascending order.

To complement this collective view, we also measure inequality from the perspective of individual behavior. For each individual $u \in U$, we compute an individual Gini index G_u , applying Equation 1 to D_u (the visits made by u). That is, we compute

the inequality in how frequently each venue is visited by the individual. The average individual Gini index is then given by:

$$\bar{G} = \frac{1}{|U|} \sum_{u \in U} G_u, \quad (2)$$

which captures the typical inequality in venue usage across individuals.

Individual perspective

From the individual perspective, we construct a co-location network in which nodes represent individuals and edges indicate co-presence at the same venue within a specified time window. Intuitively, this network captures how individuals encounter one another through shared spatial activity in the city.

Formally, let $D = (u_i, v_j, t_k)$ be the dataset of individual–venue visits. Given a time window $[t_1, t_2]$, the co-location network is defined as an undirected graph $G = (U', E)$, where $U' \subseteq U$ is the set of individuals active in that time window (i.e., who move at least once), and $(u_m, u_n) \in E$ if and only if individuals u_m and u_n visited the same venue v_j within the time window. That is $\exists (u_m, v_j, t_k), (u_n, v_j, t_l) \in D$ such that $t_k, t_l \in [t_1, t_2]$.

To investigate the presence of hierarchical structure in the social interactions encoded by the co-location network, we analyze the tendency of high-degree nodes to form a densely interconnected core (rich club). There is substantial evidence showing that rich-club structures can influence the dynamics of complex systems (Pedreschi et al. 2022; Bertagnoli and De Domenico 2022; Berahmand et al. 2018; Colizza et al. 2006), such as fostering socio-economic development (Kang et al. 2022) and shaping the spatial organization of cities (Jia et al. 2022).

Following the method proposed by Zhou and Mondragón (2004), we identify the set U_{rich} as the h nodes with the highest degree in G , and compute the rich-club density as the ratio of the number of actual links among U_{rich} to the maximum possible number of links in a complete subgraph of h nodes, i.e., $\frac{h(h-1)}{2}$.

We also examine how the degree distribution of social interactions may be affected by the influence of the recommender system. Given that the degree distribution $P(k)$ in real-world networks often exhibits heavy-tailed behavior, we fit a linear regression to the log-log plot of $P(k)$ derived from the co-location network G , and report the absolute value of the slope of the fitted line, denoted by α . Larger values of α correspond to a steeper decline, reflecting a distribution closer to exponential decay, whereas smaller values reflect a more uniform structure. We estimate $P(k)$ using the empirical degree distribution, defined as $P(k) = \frac{|\{u \in U' : \deg(u) = k\}|}{|U'|}$, where $\deg(\cdot)$ denotes the degree of a node in G .

4 Experimental settings

In this section, we describe the experimental settings used in our study. Section 4.1 presents the recommendation systems evaluated in our simulations. Section 4.2 details the dataset on which our experiments are based, and Section 4.3 outlines the values and configurations of parameters used in the simulation framework.

4.1 Benchmark recommenders

Various recommender systems have been designed to assist and augment users in discovering the most relevant and valuable content (Ricci et al. 2021a,b). Among the various approaches, collaborative filtering represents one of the most widely adopted families of algorithms, as it relies solely on binary feedback indicating whether a user has interacted with a particular item (Koren et al. 2021). These techniques have also been successfully applied to the recommendation of venues in urban settings (Rahmani et al. 2022a), consistently achieving high accuracy across benchmark datasets for next-venue recommendation.

We benchmark several recommendation models spanning classical neighborhood-based methods, matrix factorization techniques, deep generative models, geographical recommenders, and graph neural network-based approaches. The list of models included in our study is detailed below:

- **User-KNN** (Aiolli 2013): Neighborhood-based method that recommends items based on the preferences of users with similar interaction histories;
- **Item-KNN** (Aiolli 2013): Similar to User-KNN, but recommends items that are similar to those the user has previously interacted with;
- **Matrix Factorization (MF)** (Sarwar et al. 2000): Model-based approach that decomposes the user-item interaction matrix into latent user and item feature vectors, enabling prediction of missing interactions;
- **Bayesian Personalized Ranking (BPRMF)** (Rendle et al. 2009): Extension of matrix factorization that optimizes for pairwise ranking by assuming users prefer observed items over unobserved ones, and learning to rank accordingly;
- **Multinomial Variational Autoencoder (MultiVAE)** (Liang et al. 2018): Generative model based on deep learning that captures user preferences by learning a probabilistic latent space using variational inference;
- **Light Graph Convolutional Network (LightGCN)** (He et al. 2020): Recommendation system based on graph neural networks that propagates user and item embeddings over a user-item bipartite graph;
- **PGN** (Sánchez and Dietz 2022): Hybrid approach that averages the scores of User-KNN, a popularity-based recommender, and a geographical model that suggests venues near the centroid of the user’s previously visited locations.

As different models exhibit varying levels of bias in venue recommendation (Rahmani et al. 2022b), and algorithmic bias is directly linked to the long-term effects of feedback loops (Mansoury et al. 2020; Chaney et al. 2018), our comprehensive evaluation is designed to capture the different behavioral shifts and inequality patterns that may emerge from each recommendation strategy over time. Details about the hyperparameters and the training procedure of all the algorithms are in Appendix B. As a sanity check, we report the performance of all the recommenders trained on D_{train} and tested on D_{post} in terms of $\text{HitRate}@20$ and $mRR@20$, see Table B1 in Appendix B.

4.2 Dataset

We use a Foursquare dataset that contains mobility data from New York City collected over approximately 10 months, from April 3, 2012, to February 16, 2013 (304 days) [Yang et al. \(2014\)](#). This dataset comprises 227,428 check-ins, each annotated with a timestamp, GPS coordinates, and fine-grained venue categories.

For consistency, we assign a single category to each venue, selecting the *Second Category* level as it provides a balanced granularity between the broader *First Category* and the highly specific *Third Category*³. To ensure a more realistic scenario reflecting human adoption of AI-assisted mobility, we apply several preprocessing steps. Specifically, we remove check-ins to categories representing familiar locations (e.g., *Office*, *Home*, *Meeting Room*), modes of transportation (e.g., *Train*, *Ferry*, *Road*), and venues labeled with *Unknown* categories. Appendix C provides the list of excluded categories.

After preprocessing, the dataset contains 166,306 check-ins from 1,083 unique users to 23,459 unique venues spanning 159 distinct categories. On average, each category includes approximately 172 venues. In our simulations, we set $T_{\text{train}} = 210$ days and $T_{\max} = 304$ days.

4.3 Parameter settings

Our simulation framework relies on a set of parameters that govern the behavioral rules of the agents involved. Table 1 summarizes the symbols used, their corresponding meanings, and the values adopted throughout the simulations. Our framework requires only three parameters, aligning with our goal of assessing the effect of recommendation systems on urban dynamics with minimal changes to all other factors, thereby isolating the impact of algorithmic intervention.

Table 1: Simulation parameters adopted in our framework.

η	adoption rate	$\{0.0, 0.2, 0.4, 0.6, 0.8, 1.0\}$
Δ	retraining frequency	7 days
p	exploration probability	$0.6 \times V ^{-0.21}$ (Song et al. 2010)

The adoption rate η is a crucial parameter in our framework. To systematically investigate the effects of recommendation systems, we vary η across a predefined grid of values ranging from 0 to 1, with step size of 0.2.

The parameter Δ reflects how frequently the recommendation system is updated (retrained) to account for the evolving nature of user preferences. We set $\Delta = 7$ days, meaning the recommender is retrained weekly to follow the dynamics introduced by the human-AI feedback loop.

When a human agent does not rely on the recommender system, it follows the EPR model introduced by [Song et al. \(2010\)](#). Empirical analyses in [Song et al. \(2010\)](#)

³<https://observablehq.com/d/94b009d907d7c023>

confirm the model’s ability to reproduce the scaling properties of human mobility, capturing the balance between returning to familiar locations and exploring new ones. This dual behavioral perspective has been validated on real-world data, where the probability of exploring a new venue is given by $p = \rho \times |V|^{-\gamma}$, with $|V|$ denoting the number of unique venues. The parameters ρ and γ were estimated on empirical datasets and set to 0.6 and 0.21, respectively.

5 Results

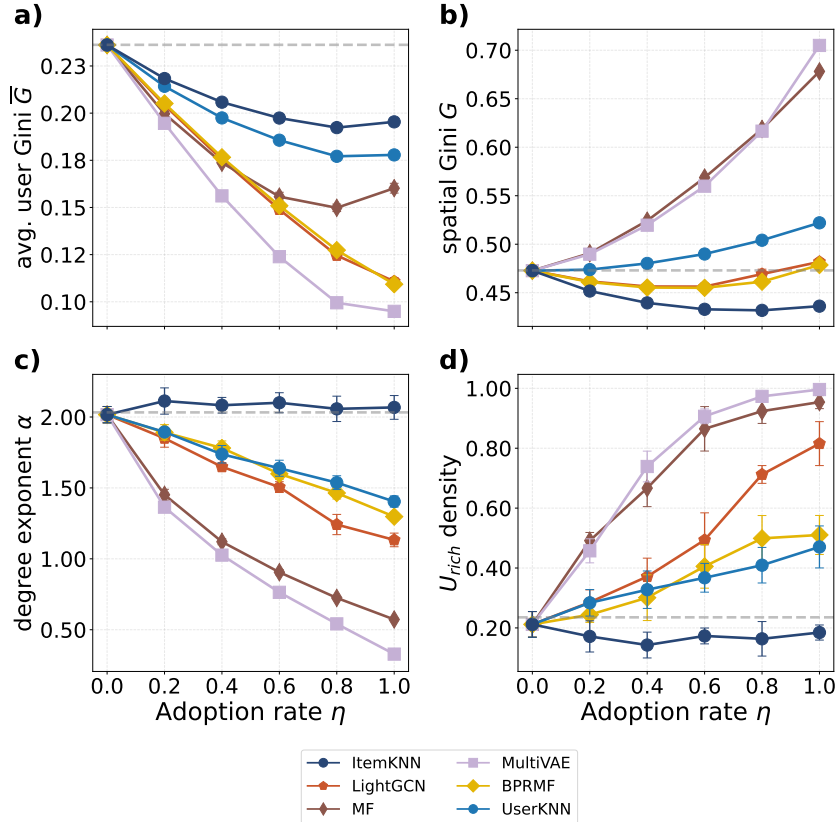


Fig. 2: Effects of recommender system adoption η . (a) Average individual Gini coefficient \bar{G} ; (b) Gini coefficient of the distribution of visits across venues G ; (c) Power-law exponent of the co-location network’s degree distribution α ; (d) Internal density of the rich club (top 15 nodes by degree) in the co-location network. Each curve is an algorithm; each points represents the average over five simulation runs.

Figure 2 compares the effects of different recommendation systems as a function of the adoption rate η . All values are averaged over five independent simulation runs.

Figures 2a and 2b report the average individual Gini coefficient \bar{G} and the collective Gini coefficient G of venue visits, respectively. We remind that the former captures how evenly each individual distributes their visits across venues, while the latter reflects overall disparities in venue popularity.

For clarity sake, we do not report results for the PGN recommender in the main text, as they closely mirror the patterns observed for MF and MultiVAE. A more detailed comparison, including PGN, is provided in Appendix D.

All recommender systems reduce \bar{G} compared to the baseline with no recommendations ($\eta = 0$, dashed line at $\bar{G} \approx 0.2$ in Figure 2a), and the effect intensifies with increasing η . While ItemKNN and UserKNN yield modest reductions, the deep learning-based models – BPRMF, LightGCN, and MultiVAE – produce significantly stronger decreases in \bar{G} . Notably, for $\eta = 1$ (full reliance on the recommender system), MultiVAE achieves a value of $\bar{G} \approx 0.09$, corresponding to a relative reduction of approximately 60% compared to $\eta = 0$. This finding indicates that, under algorithmic influence, individual diversity increases: as individuals depend more on recommender systems for deciding where to go, they tend to explore a wider and more varied range of venues instead of focusing on just a few.

Key Result 1

Recommender systems boost individual diversity, as reflected by a consistent drop in average individual Gini across all models.

However, this increase in individual diversity does not imply a more diverse collective behaviour. Indeed, the collective Gini coefficient G increases with η for some recommenders (see Figure 2b). UserKNN, MF, and MultiVAE all lead to a sharp increase in G as adoption increases. Notably, for $\eta = 1$, MultiVAE reaches $G = 0.7$, representing an increase of approximately 47% compared to $\eta = 0$, indicating a more uneven distribution of visits across venues. Deep-learning-based algorithms such as LightGCN and BPRMF slightly reduce inequality, except for full-adoption scenarios. ItemKNN is the only model that slightly but consistently reduces global inequality compared to the baseline, reaching $G \approx 0.44$, which corresponds to a relative reduction of approximately 7% compared to $\eta = 0$. These results suggest that a systematic increase in individual diversity may be accompanied by a simultaneous concentration of visits on a smaller subset of venues.

Key Result 2

More individual diversity does not imply more collective diversity: as individuals explore more, visits may concentrate on a few popular venues.

Analysis of the co-location network shows that all recommender systems, except ItemKNN, lead to an increase in the exponent α of the power-law degree distribution, with the effect particularly pronounced for MultiVAE and MF (see Figure 2c). A lower α indicates a flatter distribution, meaning co-location ties are more evenly spread across individuals, rather than concentrated around a few highly connected

ones. Thus, most recommenders reduce the skewness of the co-location structure, promoting broader interpersonal mixing. Regarding ItemKNN, as the adoption rate η increases, the exponent α remains close to the baseline, indicating little change in user co-presence patterns (squares in Figure 2c).

A similar pattern is observed in the rich-club structure U_{rich} , defined as the top 15 individuals with the highest degree in the co-location network. For all recommender systems except ItemKNN, the internal density of connections within this group – the ratio of observed to possible links – increases sharply with higher values of η , approaching nearly 1 for MultiVAE (see Figure 2d). This suggests that highly connected individuals increasingly tend to co-locate with one another. In contrast, for ItemKNN, the rich-club density remains close to the baseline level of approximately 0.2, indicating little change in elite clustering.

Key Result 3

Recommender systems promote broader mixing of co-locations, while rich-club individuals become nearly fully connected in the co-location network.

Venue Perspective

Since MultiVAE and ItemKNN represent the two extreme cases across all the metrics discussed, we provide a more detailed analysis of the patterns that emerge from their adoption within our framework. The contrasting spatial effects of MultiVAE and ItemKNN are illustrated in Figures 3 and 4, which show both individual and collective patterns under the extreme cases of null and full adoption ($\eta = 0$ and $\eta = 1$). Similar analysis for all other recommended systems are in the Supplementary Material.

MultiVAE

For MultiVAE, Figure 3a-b shows the spatial distribution of visits for a representative individual (User 900). Under the scenario of no recommendation ($\eta = 0$), visits are mostly concentrated on just two venues in western Midtown Manhattan (Figure 3a). Under full adoption ($\eta = 1$), the activity of User 900 becomes more spatially dispersed, with visits more evenly distributed across the city (Figure 3b). This shift is captured by the individual Gini coefficient, which drops from $G_u = 0.41$ to $G_u = 0.19$ – a reduction of approximately 54% – with a consistent decline observed as the adoption rate η increases (Figure 3c).

At the collective level, MultiVAE shows the opposite effect. Figure 3d-e shows the aggregated spatial distribution of visits for a sample of 250 users. When $\eta = 0$, visits are relatively uniformly spread across the city, including peripheral neighborhoods and outer boroughs, with $G = 0.32$. When $\eta = 1$, visits become concentrated in a small number of venues, especially in Midtown and Lower Manhattan. The Gini coefficient increases to $G = 0.50$, marking a 56% rise in venue popularity inequality (see Figure 3f). These results confirm the results shown in the previous section: while MultiVAE promotes more balanced behaviour at the individual level, it drives convergence toward a narrow set of highly frequented locations at the collective level, reinforcing popularity inequality.

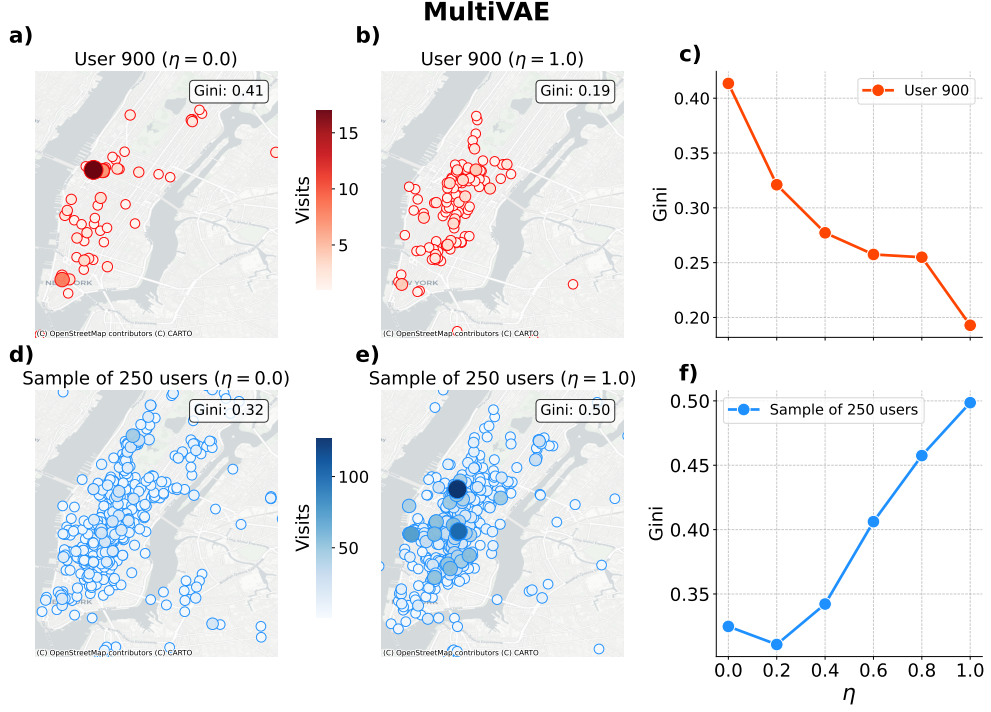


Fig. 3: Venue visitation patterns under MultiVAE for null ($\eta=0$) and full ($\eta=1$) adoption. (a–b) Geographical distribution of visits by a representative user (User 900). Visit intensity is proportional to point size and color. When $\eta=1$, visits become more evenly distributed across venues, with the individual Gini coefficient decreasing from $G_u=0.41$ to $G_u=0.19$. (c) Individual Gini coefficient for User 900 as a function of η , showing a consistent decline. (d–e) Aggregated venue visits for a sample of 250 users. When $\eta=1$, visits are more concentrated in a few high-traffic venues, particularly in central Manhattan. (f) Gini coefficient of venue visit distribution across the sample, rising from $G=0.32$ to $G=0.50$ with increasing η .

ItemKNN

In contrast, ItemKNN produces more stable spatial dynamics (see Figure 4). For User 900, the shift from $\eta = 0$ to $\eta = 1$ results in a slightly more balanced, yet still unequal, visitation pattern (see Figure 4a–b). The individual Gini coefficient decreases from $G_u = 0.41$ to $G_u = 0.37$, a reduction of approximately 9.8%, with only minor fluctuations across η (Figure 4c). At the collective level, ItemKNN contributes to a small improvement in spatial balance. Figure 4d–e shows that the city-wide distribution of visits remains fairly dispersed across both conditions. The Gini coefficient decreases from $G = 0.32$ to $G = 0.27$ under full adoption (Figure 4f confirms this downward trend). Unlike MultiVAE, ItemKNN does not induce spatial convergence toward a limited set of venues. Instead, it preserves heterogeneity in mobility patterns while slightly improving overall equity in how urban space is visited.

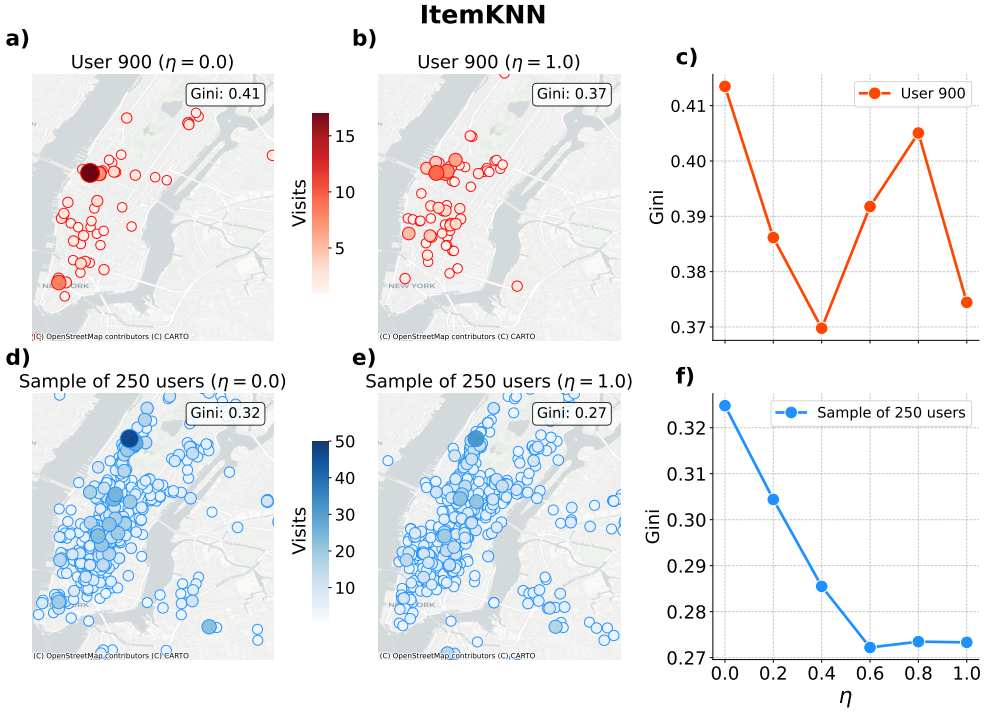


Fig. 4: Figure 4. Venue visitation patterns under ItemKNN for null ($\eta=0$) and full ($\eta=1$) adoption. (a–b) Geographical distribution of visits by a representative user (User 900). A modest shift toward a more balanced visitation pattern is observed, with the individual Gini decreasing from $G_u=0.41$ to $G_u=0.37$. (c) Individual Gini coefficient for User 900 as a function of η , showing minor fluctuations. (d–e) Aggregated venue visits for a sample of 250 users. Visit distributions remain fairly dispersed under both conditions. (f) Gini coefficient of venue visit distribution across the sample, decreasing slightly from $G=0.32$ to $G=0.27$.

Individual Perspective

MultiVAE

MultiVAE substantially reshapes the structure of urban co-presence (see Figure 5). We remind that, in the co-location network, two individuals are linked if they visit the same venue within the same epoch of the simulation. Figure 5a,c shows the degree distributions of the co-location network under the two extreme cases of null and full adoption ($\eta = 0$ and $\eta = 1$). Under the autonomous choice scenario ($\eta = 0$), the degree distribution follows a steeper power-law decay, with a median degree of 4 and exponent $\alpha \approx 2.0$ (Figure 5a). When users fully adopt MultiVAE ($\eta = 1$), the degree distribution flattens significantly, with a heavier tail and a substantial increase in median degree (Figure 5c). Notably, the number of nodes in the network also increases, which implies broader participation in the social layer under algorithmic influence.

Figure 5d,f offers a visual snapshot of the co-location network structure under the null and full adoption scenarios for MultiVAE. The inner red nodes denote the rich club and the peripheral nodes lie along the outer circle. When $\eta = 0$, the peripheral subnetwork is sparse (Peripheral Density, PD is almost 0) and the rich club is weakly connected (Rich-club Density, RD ≈ 0.10). When $\eta = 1$ with MultiVAE, the structure shifts dramatically: peripheral nodes become more interconnected ($PD \approx 0.12$) and the rich club much more densely connected ($RD \approx 0.64$), forming a dense social core.

These structural shifts in co-location patterns are tightly connected to changes in venue popularity. Figure 5g reports the rank-size distribution of venue visits. With full adoption of MultiVAE, the head of the distribution grows significantly: a few venues receive disproportionately high attention, reflecting an increase in spatial centralization. This dynamic reinforces not only high-degree users but also high-frequency venues, suggesting that popular places become even more dominant. This pattern is further confirmed in Figure 5h, which reports the Lorenz curves of visit distributions under different scenarios. The curve for MultiVAE with $\eta = 1$ deviates more strongly from the equality line, indicating higher overall inequality in venue visitation, despite the increased uniformity in individual user behaviour and co-location degree.

ItemKNN

In contrast to MultiVAE, ItemKNN has a minimal effect on the structure of the co-location network and the distribution of visits across venues. Figure 5a,b shows the degree distributions of the co-location network under $\eta = 0$ and $\eta = 1$ with ItemKNN, respectively. Both distributions follow similar power-law trends, with nearly identical slopes ($\alpha \approx 2.0$ and $\alpha \approx 2.1$) and a stable median degree of 4. This indicates that ItemKNN does not substantially alter the topology of social co-presence: individuals maintain similar numbers of co-located interactions regardless of whether they follow the algorithm's suggestions.

A structural view of the co-location network confirms this stability. Figure 5d,e visualizes the rich-club structure under the null adoption and full adoption with ItemKNN. In both cases, the peripheral density remains at zero ($PD \approx 0.00$), and the rich-club density remains almost constant ($RD = 0.09$ and $RD \approx 0.09$ respectively). This suggests that ItemKNN neither strengthens the elite core of highly connected individuals nor promotes wider cohesion among peripheral ones.

The implications from a venue perspective are shown in Figure 5g-h. The rank-size distribution of venue visits (Figure 5g) shows that ItemKNN largely preserves the pattern of venue visits across adoption levels, with only minor variation in the long tail. The Lorenz curves (Figure 5h) reveal a slight shift toward greater equality under full adoption of ItemKNN, as its curve moves marginally closer to the diagonal compared to the null adoption scenario. This indicates a modest reduction in the inequality of venue visits, although the overall pattern remains similar. Overall, ItemKNN preserves the existing structure of user interactions and venue usage. Unlike more complex algorithms, it avoids concentrating visits or reinforcing strong social cores, instead maintaining a relatively stable distribution of co-location and visits across the system.

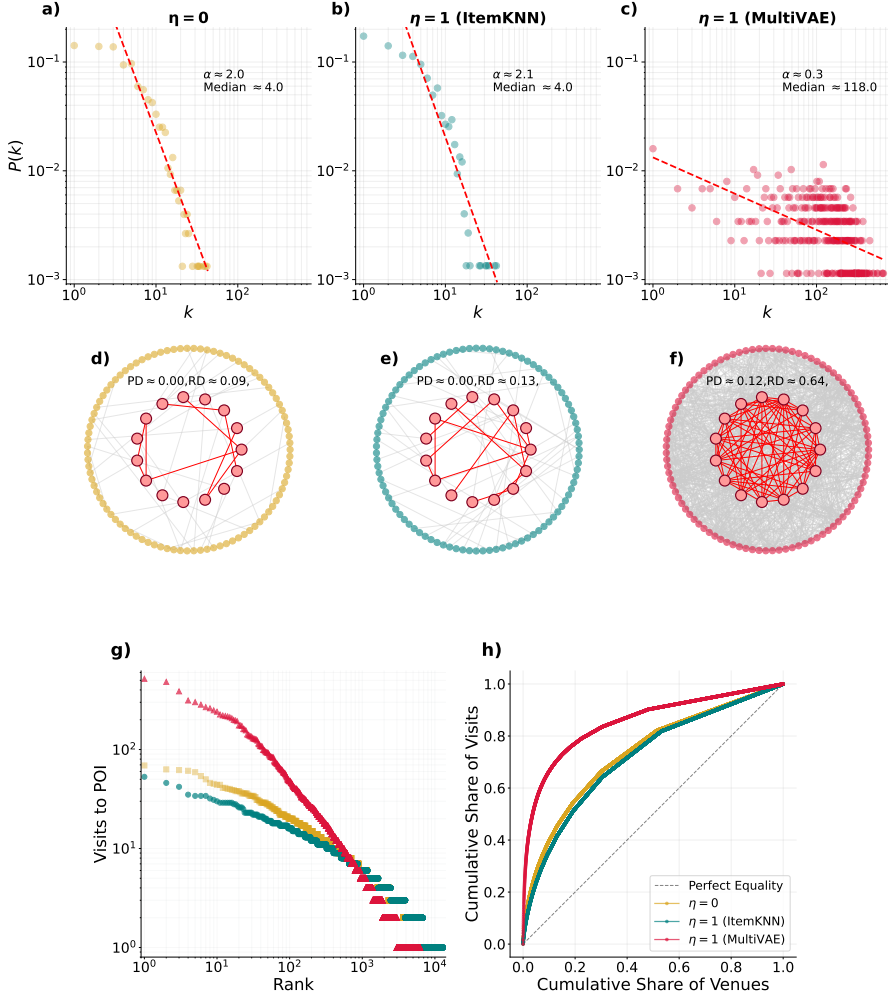


Fig. 5: Social and venue level effects of algorithms under null ($\eta=0$) and full ($\eta=1$) adoption. (a-c) Degree distribution of the co-location network, for null adoption, full adoption with ItemKNN and full adoption with MultiVAE. MultiVAE significantly flattens the distribution and increases median degree, while ItemKNN maintains the original network structure. (d-f) Visualization of the co-location network (sampled), highlighting the rich-club structure (red nodes) and peripheral nodes (circular layout) for null adoption, full adoption with ItemKNN and full adoption with MultiVAE. Rich-club density increases dramatically for MultiVAE, while remaining constant for ItemKNN. (g-h) Rank-size distribution and Lorenz curves of venue visits: under $\eta=1$ for MultiVAE, top-ranked venues receive disproportionately more visits.

5.1 Understanding the individual-collective diversity trade-off

The recommender systems we analyzed reduce inequality in how individual individuals distribute their visits across venues, yet most of them simultaneously increase the inequality in how visits are distributed across venues at the collective level. How can these two seemingly contradictory mechanisms coexist?

To address this question, we compare individuals' exploratory visits during the simulation to those recorded in the historical training data (D_{train}). We model the interaction between individuals and venues as a bipartite network, where one set of nodes represents individuals, the other represents venues, and edges correspond to visits. We construct two such networks: one based on the historical training data, and another based on exploratory visits simulated under full algorithmic adoption ($\eta = 1$). In the training network, an edge connects an individual to a venue if it was visited during the training period. In the simulation network, an edge is added only if the individual visited a venue for the first time, i.e., a venue not in D_{train} .

We focus on MultiVAE, which exhibits the strongest impact on inequality patterns. To analyze attention across venue popularity, we group venues into deciles based on their number of unique visitors in the training set. Each decile represents 10% of venues, ranked from least (decile 1) to most popular (decile 10).

The degree of a venue reflects how many users visited it. Since we model binary interactions, the degree is equivalent to the weighted degree. To normalize across the network, we compute the normalized weighted degree for each venue v :

$$\hat{d}_v = \frac{d_v}{\sum_{v' \in \mathcal{V}} d_{v'}} \quad (3)$$

We then aggregate these values within each decile to compute the share of attention directed to that group:

$$\hat{D}_g = \sum_{v \in g} \hat{d}_v \quad (4)$$

This measure, \hat{D}_g , captures the fraction of all user–venue interactions involving venues in group g .

Figure 6a shows that, while the most popular venues (decile 10) already attract the largest share of attention (33.0%) in the training data, the distribution is relatively balanced, with other deciles also receiving a meaningful portion of visits. After the simulation, under the influence of MultiVAE, attention becomes far more concentrated (see Figure 6b): decile 10 captures 56.91% of all interactions in the exploration phase. This comes at the expense of nearly every other decile, whose shares decline.

To quantify this shift, we compute the change in attention share for each decile between the training and exploration phases: $\delta_g = \hat{D}_g^{(\text{simulation})} - \hat{D}_g^{(\text{train})}$. As shown in Figure 7, the shift is stark: decile 10 gains over 20 percentage points in attention, while all other deciles, especially the least popular ones, lose ground.

The analysis shows that the new venues visited by individuals – those driving the increase in individual diversity – are often the same across the population, typically the most popular ones. This reflects a rich-get-richer dynamic: while individual-level diversity improves, it does so by directing many individuals toward a narrow set of

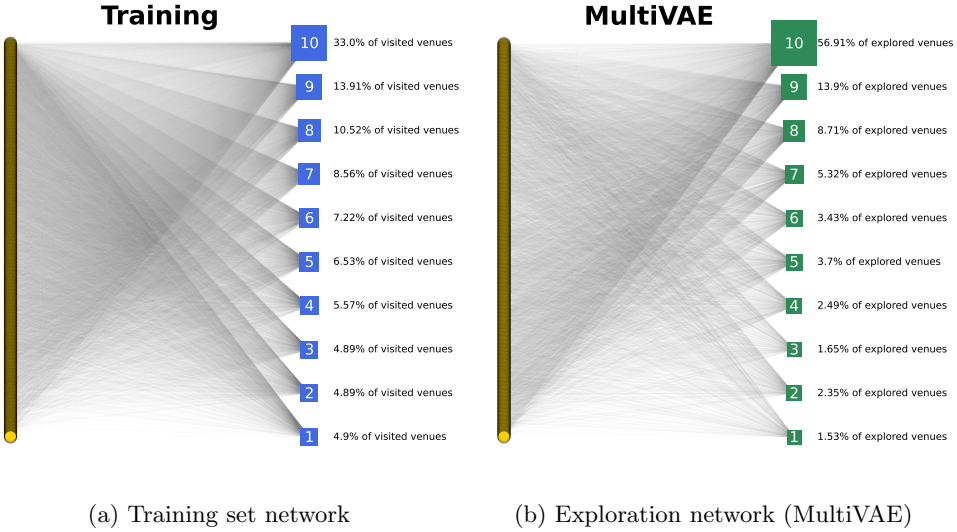


Fig. 6: Bipartite individual–venue networks. Individuals are on the left; venue deciles are on the right. Each decile contains 10% of venues, ranked by popularity in the training data. Percentages indicate each decile’s share of total individual–venue interactions. In the training network (left), an edge indicates a visit during the training period. In the exploration network (right), an edge represents a simulated visit to a venue not seen during training (i.e., a novel exploration). Venues with fewer than 3 unique visitors are excluded.

highly recommended venues. As a result, the system becomes more centralized, amplifying popularity bias and revealing a fundamental tension: recommendation systems can enhance fairness at the individual level while undermining it collectively.

Key Result 4

Individual diversity rises mostly through visits to the same popular venues.

6 Discussion

Our findings contribute to the growing body of research on human–AI ecosystems by extending the analysis of feedback loops to the domain of urban mobility. In what follows, we interpret our results through the lens of the field of human mobility and the emerging debate on human–AI coevolution (Pedreschi et al. 2025), i.e., how to measure and model the reciprocal influence between human behavior and algorithmic systems, and how this feedback shapes the dynamics of complex systems.

Our main result is that, for most recommendation algorithms, the feedback loop leads to a divergence between individual and collective diversity. On the one hand, individuals tend to distribute their visits more evenly across venues, resulting in increased

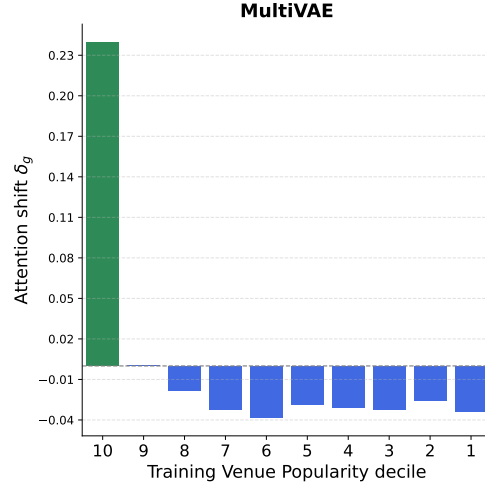


Fig. 7: Change in normalized weighted degree across venue popularity deciles (1–10). Bars show the difference in share of interactions between exploration and training under MultiVAE.

individual diversity. On the other hand, the collective flows of people become more concentrated, with a small set of venues attracting a disproportionate share of total visits – a decreased collected diversity. These two apparently contrasting mechanisms coexist because individual diversity rises mostly through visits to the same popular venues. This trade-off mirrors patterns observed in other human-AI ecosystems (Papalardo et al. 2024). In online retail, for example, recommender systems often increase individual exposure to niche items while amplifying popularity bias at the aggregate level—leading to market concentration around top-ranked products (Lee and Hosanagar 2019; Fleder and Hosanagar 2009). A similar dynamic has been observed in the use of generative AI: while it can enhance individual creativity, as shown by online experiments (Doshi and Hauser 2024), it tends to reduce collective diversity, especially under repeated feedback loops, which may lead to mode collapse and homogenized outputs at scale (Shumailov et al. 2024). Our results suggest that such structural imbalances are not unique to digital content but extend to physical movement patterns in cities. This raises important concerns about the long-term effects of algorithmic mediation on urban accessibility, spatial inequality, and the viability of less popular or peripheral venues.

Moreover, our findings challenge the core assumptions of many mechanistic models of human mobility, such as the Exploration and Preferential Return (EPR) model used in this study (Song et al. 2010). These models generally assume that individuals make movement decisions autonomously, choosing whether to return to familiar locations or explore new ones based on internal behavioral rules. Yet, in contemporary urban environments, such decisions are increasingly mediated by algorithmic suggestions. As our results show, recommender systems can significantly reshape individual

mobility patterns, with downstream effects on venue popularity and patterns of co-location. These findings suggest that classical mobility models must be revised and extended to explicitly account for algorithmic influence as a primary driver of behavior. Incorporating this dimension will lead to more realistic representations of mobility in the algorithmically guided city and support the development of systems that better reflect societal goals such as fairness, accessibility, and sustainability.

7 Conclusion

In this article, we modeled the human–AI feedback loop in the context of next-venue recommendation and introduced a simulation framework to assess its impact on individual mobility behavior, venue popularity, and co-location patterns. By experimenting with a range of recommender system types on real-world venue visit data from New York City, we found a consistent trend: individual visitation diversity increases, while collective diversity decreases, indicating a growing concentration of attention on a smaller set of venues.

This work has some limitations. First, our modeling of the feedback loop is based on simulation rather than direct observation, due to the lack of access to real-time platform data such as recommendation outputs and user interactions. As a result, our findings should be understood as a what-if analysis, exploring hypothetical scenarios rather than providing empirical evidence. We hope that regulatory initiatives like the Digital Services Act will promote greater transparency and data access, enabling researchers to conduct controlled experiments directly on digital platforms and rigorously assess the real-world impact of recommender systems on urban dynamics. Second, individual decision-making is modeled using simplified probabilistic rules, which may not capture the full complexity of real-world behavior. Finally, our experiments are limited to a single urban context, so the generalizability of the results to other cities with different spatial or social structures remains to be explored.

Despite these limitations, our work opens several directions for future research. One promising avenue is to study more deeply the role of the retraining period, investigating how the frequency and timing of algorithm updates affect the long-term evolution of mobility patterns and urban inequalities. Another direction is to design impact-aware recommender systems that monitor their own influence on the urban environment and adapt accordingly; for instance, by promoting less popular venues when a concentration bias is detected. Finally, the model of autonomous decision-making could be enriched by integrating more sophisticated mechanistic models of human mobility, capturing factors such as temporal routines, social interactions, or multi-modal transportation behaviors.

Reproducibility and Code

Our framework and analysis are fully reproducible, with all code available at <https://github.com/mauruscz/UrbanFeedbackLoop>.

The simulations were executed on high-performance computing platforms with 64 CPU cores (AMD EPYC 7313 16-Core Processor) and \sim 1.18 TB RAM. While the simulations are computationally intensive, we implemented a highly parallelized and

modular architecture to optimize performance and resource utilization. Experiments with neural recommenders, i.e., MultiVAE, LightGCN, BPRMF, have been conducted on a DGX Server equipped with 4 NVIDIA Tesla V100 GPU (32GB) and CUDA Version 12.2.

Authors' contributions. GM and MM implemented the simulations, the data analysis, and developed the code. GM, MM, and LP conceived the figures. GM made the plots. GM, MM and LP wrote the paper. LP directed and supervised the research. All authors contributed to the scientific discussion, read and approved the paper.

Acknowledgements. Giovanni Mauro has been supported by SoBig-Data.it—Strengthening the Italian RI for Social Mining and Big Data Analytics”, prot. IR0000013, avviso n. 3264 on 28/12/2021. Marco Minici acknowledges partial support by (*i*) the SERICS project (PE00000014) under the NRRP MUR program funded by the EU - NGEU and (*ii*) “SoBig-Data.it - Strengthening the Italian RI for Social Mining and Big Data Analytics” - Prot. IR0000013, avviso n. 3264 on 28/12/2021. Luca Pappalardo has been supported by PNRR (Piano Nazionale di Ripresa e Resilienza) in the context of the research program 20224CZ5X4_PE6_PRIN 2022 “URBAI – Urban Artificial Intelligence” (CUP B53D2301277006), funded by European Union – Next Generation EU.

We thank Daniele Fadda for the invaluable help with the data visualizations.

References

- Afèche P, Liu Z, Maglaras C (2023) Ride-hailing networks with strategic drivers: The impact of platform control capabilities on performance. *Manuf Serv Oper Manag* 25(5):1890–1908
- Aiolli F (2013) Efficient top-n recommendation for very large scale binary rated datasets. In: Proceedings of the 7th ACM conference on Recommender systems, pp 273–280
- Arora N, Cabannes T, Ganapathy S, et al (2021) Quantifying the sustainability impact of google maps: A case study of salt lake city. *CoRR* abs/2111.03426
- Berahmand K, Samadi N, Sheikholeslami SM (2018) Effect of rich-club on diffusion in complex networks. *International Journal of Modern Physics B* 32(12):1850142
- Bertagnolli G, De Domenico M (2022) Functional rich clubs emerging from the diffusion geometry of complex networks. *Physical Review Research* 4(3):033185
- Bokányi E, Hannák A (2020) Understanding Inequalities in Ride-Hailing Services Through Simulations. *Scientific Reports* 10(1):6500
- Boratto L, Fenu G, Marras M (2021) Connecting user and item perspectives in popularity debiasing for collaborative recommendation. *Information Processing & Management* 58(1):102387

- Chaney AJ, Stewart BM, Engelhardt BE (2018) How algorithmic confounding in recommendation systems increases homogeneity and decreases utility. In: Proceedings of the 12th ACM conference on recommender systems, pp 224–232
- Chen J, Dong H, Wang X, et al (2023) Bias and debias in recommender system: A survey and future directions. *ACM Transactions on Information Systems* 41(3):1–39
- Colizza V, Flammini A, Serrano MA, et al (2006) Detecting rich-club ordering in complex networks. *Nature physics* 2(2):110–115
- Cornacchia G, Böhm M, Mauro G, et al (2022) How routing strategies impact urban emissions. In: Proceedings of the 30th International Conference on Advances in Geographic Information Systems, pp 1–4
- Cornacchia G, Nanni M, Pappalardo L (2023) One-shot traffic assignment with forward-looking penalization. In: SIGSPATIAL/GIS. ACM, pp 87:1–87:10
- Cornacchia G, Lemma L, Pappalardo L (2024) Alternative routing based on road popularity. In: Proceedings of the 2nd ACM SIGSPATIAL Workshop on Sustainable Urban Mobility. Association for Computing Machinery, New York, NY, USA, SUMob '24, p 14–17, <https://doi.org/10.1145/3681779.3696836>, URL <https://doi.org/10.1145/3681779.3696836>
- Doshi AR, Hauser OP (2024) Generative ai enhances individual creativity but reduces the collective diversity of novel content. *Science Advances* 10(28):eadn5290
- Edelman BG, Luca M (2014) Digital discrimination: The case of airbnb. com. Harvard Business School NOM Unit Working Paper (14-054)
- Elahi M, Kholgh DK, Kiarostami MS, et al (2021) Investigating the impact of recommender systems on user-based and item-based popularity bias. *Information Processing & Management* 58(5):102655
- Ensign D, Friedler SA, Neville S, et al (2018) Runaway feedback loops in predictive policing. In: Friedler SA, Wilson C (eds) Proceedings of the 1st Conference on Fairness, Accountability and Transparency, Proceedings of Machine Learning Research, vol 81. PMLR, pp 160–171, URL <https://proceedings.mlr.press/v81/ensign18a.html>
- Fleder D, Hosanagar K (2009) Blockbuster culture's next rise or fall: The impact of recommender systems on sales diversity. *Management science* 55(5):697–712
- Gonzalez MC, Hidalgo CA, Barabasi AL (2008) Understanding individual human mobility patterns. *nature* 453(7196):779–782
- He X, Deng K, Wang X, et al (2020) Lightgcn: Simplifying and powering graph convolution network for recommendation. In: Proceedings of the 43rd International ACM SIGIR conference on research and development in Information Retrieval, pp 639–648

- Jia T, Cai C, Li X, et al (2022) Dynamical community detection and spatiotemporal analysis in multilayer spatial interaction networks using trajectory data. *International Journal of Geographical Information Science* 36(9):1719–1740
- Jiang R, Chiappa S, Lattimore T, et al (2019) Degenerate feedback loops in recommender systems. In: Proceedings of the 2019 AAAI/ACM Conference on AI, Ethics, and Society. Association for Computing Machinery, New York, NY, USA, AIES ’19, p 383–390, <https://doi.org/10.1145/3306618.3314288>, URL <https://doi.org/10.1145/3306618.3314288>
- Kang C, Jiang Z, Liu Y (2022) Measuring hub locations in time-evolving spatial interaction networks based on explicit spatiotemporal coupling and group centrality. *International Journal of Geographical Information Science* 36(2):360–381
- Koolwal V, Mohbey KK (2020) A comprehensive survey on trajectory-based location prediction. *Iran Journal of Computer Science* 3(2):65–91
- Koren Y, Rendle S, Bell R (2021) Advances in collaborative filtering. *Recommender systems handbook* pp 91–142
- Lee D, Hosanagar K (2019) How do recommender systems affect sales diversity? a cross-category investigation via randomized field experiment. *Information Systems Research* 30(1):239–259
- Lesota O, Geiger J, Walder M, et al (2024) Oh, behave! country representation dynamics created by feedback loops in music recommender systems. In: Proceedings of the 18th ACM Conference on Recommender Systems. Association for Computing Machinery, New York, NY, USA, RecSys ’24, p 1022–1027
- Liang D, Krishnan RG, Hoffman MD, et al (2018) Variational autoencoders for collaborative filtering. In: Proceedings of the 2018 world wide web conference, pp 689–698
- Luca M, Barlacchi G, Lepri B, et al (2021) A survey on deep learning for human mobility. *ACM Computing Surveys (CSUR)* 55(1):1–44
- Luca M, Pappalardo L, Lepri B, et al (2023) Trajectory test-train overlap in next-location prediction datasets. *Machine Learning* 112(11):4597–4634
- Mansoury M, Abdollahpouri H, Pechenizkiy M, et al (2020) Feedback loop and bias amplification in recommender systems. In: Proceedings of the 29th ACM International Conference on Information & Knowledge Management. Association for Computing Machinery, New York, NY, USA, CIKM ’20, p 2145–2148, <https://doi.org/10.1145/3340531.3412152>, URL <https://doi.org/10.1145/3340531.3412152>
- Nguyen TT, Hui PM, Harper FM, et al (2014) Exploring the filter bubble: the effect of using recommender systems on content diversity. In: Proceedings of the 23rd

International Conference on World Wide Web. Association for Computing Machinery, New York, NY, USA, WWW '14, p 677–686, <https://doi.org/10.1145/2566486.2568012>, URL <https://doi.org/10.1145/2566486.2568012>

Pappalardo L, Simini F, Rinzivillo S, et al (2015) Returners and explorers dichotomy in human mobility. *Nature communications* 6(1):8166

Pappalardo L, Manley E, Sekara V, et al (2023) Future directions in human mobility science. *Nature computational science* 3(7):588–600

Pappalardo L, Ferragina E, Citraro S, et al (2024) A survey on the impact of ai-based recommenders on human behaviours: methodologies, outcomes and future directions. arXiv preprint arXiv:240701630

Pedreschi D, Pappalardo L, Ferragina E, et al (2025) Human-ai coevolution. *Artificial Intelligence* p 104244

Pedreschi N, Battaglia D, Barrat A (2022) The temporal rich club phenomenon. *Nature Physics* 18(8):931–938

Perez-Prada F, Monzón A, Valdés C (2017) Managing traffic flows for cleaner cities: The role of green navigation systems. *Energies* 10:791. <https://doi.org/10.3390/en10060791>

Quijano-Sánchez L, Cantador I, Cortés-Cediel ME, et al (2020) Recommender systems for smart cities. *Information systems* 92:101545

Rahmani HA, Deldjoo Y, Di Noia T (2022a) The role of context fusion on accuracy, beyond-accuracy, and fairness of point-of-interest recommendation systems. *Expert Systems with Applications* 205:117700

Rahmani HA, Deldjoo Y, Tourani A, et al (2022b) The unfairness of active users and popularity bias in point-of-interest recommendation. In: International Workshop on Algorithmic Bias in Search and Recommendation, Springer, pp 56–68

Rendle S, Freudenthaler C, Gantner Z, et al (2009) Bpr: Bayesian personalized ranking from implicit feedback. In: Proceedings of the Twenty-Fifth Conference on Uncertainty in Artificial Intelligence, pp 452–461

Ricci F, Rokach L, Shapira B (2021a) Recommender systems: Techniques, applications, and challenges. *Recommender systems handbook* pp 1–35

Ricci F, Rokach L, Shapira B (2021b) Recommender systems: Techniques, applications, and challenges. *Recommender systems handbook* pp 1–35

Sánchez P, Dietz LW (2022) Travelers vs. locals: the effect of cluster analysis in point-of-interest recommendation. In: Proceedings of the 30th ACM Conference on User Modeling, Adaptation and Personalization, pp 132–142

- Sarwar B, Karypis G, Konstan J, et al (2000) Application of dimensionality reduction in recommender system-a case study. In: ACM WebKDD workshop, Citeseer, pp 285–295
- Shumailov I, Shumaylov Z, Zhao Y, et al (2024) Ai models collapse when trained on recursively generated data. *Nature* 631(8022):755–759
- Song C, Koren T, Wang P, et al (2010) Modelling the scaling properties of human mobility. *Nature physics* 6(10):818–823
- Sun W, Khenissi S, Nasraoui O, et al (2019) Debiasing the human-recommender system feedback loop in collaborative filtering. In: Companion Proceedings of The 2019 World Wide Web Conference. Association for Computing Machinery, New York, NY, USA, WWW '19, p 645–651
- Tsvetkova M, Yasseri T, Pescetelli N, et al (2024) A new sociology of humans and machines. *Nature Human Behaviour* 8(10):1864–1876
- Wang Y, Tao L, Zhang XX (2025) Recommending for a multi-sided marketplace: A multi-objective hierarchical approach. *Marketing Science* 44(1):1–29
- Yang D, Zhang D, Zheng VW, et al (2014) Modeling user activity preference by leveraging user spatial temporal characteristics in lbsns. *IEEE Transactions on Systems, Man, and Cybernetics: Systems* 45(1):129–142
- Zhang S, Mehta N, Singh PV, et al (2021) Frontiers: Can an artificial intelligence algorithm mitigate racial economic inequality? an analysis in the context of airbnb. *Marketing Science* 40(5):813–820
- Zhou S, Mondragón RJ (2004) The rich-club phenomenon in the internet topology. *IEEE communications letters* 8(3):180–182
- Zhou Y, Dai S, Pang L, et al (2024) Source echo chamber: Exploring the escalation of source bias in user, data, and recommender system feedback loop. URL <https://arxiv.org/abs/2405.17998>, arXiv:2405.17998

Appendix A Fallback mechanism

The fallback mechanism is triggered when the standard venue selection process cannot return a valid result within the current constraints. During exploration, if no venue of the target category is available within the sampled radius r , the system first attempts to retrieve a venue belonging to a broader, coarser-grained category (First-Level category) within the same radius. If this broader match is also unsuccessful, the user is assigned the geographically nearest venue matching the original target category, regardless of the distance.

Similarly, during the return phase, if the user has not previously visited any venue of the specified target category, the mechanism attempts to return to a previously visited venue within the broader category. If that too fails, the system defaults to exploration mode, allowing the user to visit a new venue instead.

Appendix B Training of Recommender System

The UserKNN, ItemKNN, and PGN algorithms are fit to the training dataset using $k = 10$ nearest neighbors, while MF uses 32 latent factors. BPRMF and LightGCN are trained with the pairwise BPR loss, using a batch size of 16 and an L2 regularization term of 0.0001. MultiVAE is trained using cross-entropy loss along with a KL divergence term (coefficient set to 0.2), in a full-batch setting.

For algorithms requiring training, we track the training loss at the end of each epoch and apply early stopping if the loss does not decrease for five consecutive epochs. The total number of epochs is capped at 500, and we use the Adam optimizer with a learning rate of 0.001.

As a sanity check, we evaluate each trained model on D_{train} and D_{post} . For each user $u \in U$, we generate a top-K list of recommended venues and measure the HitRate and mean Reciprocal Rank (mRR) in predicting u 's interactions in D_{post} . We set $K = 20$ and report average HitRate and mRR across all users.

Table B1: Performance Metrics for Various Recommender Models

Model	HitRate@20	mRR@20
UserKNN	0.1726	0.0576
ItemKNN	0.1703	0.0377
MF	0.1870	0.0474
BPRMF	0.2261	0.0611
MultiVAE	0.1898	0.0656
LightGCN	0.2774	0.0838
PGN	0.2156	0.0704

The performance of the various recommender models we employed aligns well with findings reported in the literature [Rahmani et al. \(2022a\)](#). Our evaluation metrics are significantly higher—up to three times greater—than those typically observed. This improvement can be attributed, in part, to our methodology, which considers the venue category before invoking the recommender system.

Appendix C Dataset

We excluded all check-ins to venues with following categories: Train, Transport Hub, Transportation Service, Travel and Transportation, Boat or Ferry, Platform, Road, Island, River, Housing Development, Meeting Room, Conference Room, Office, Home (private), Apartment or Condo and Unknown.

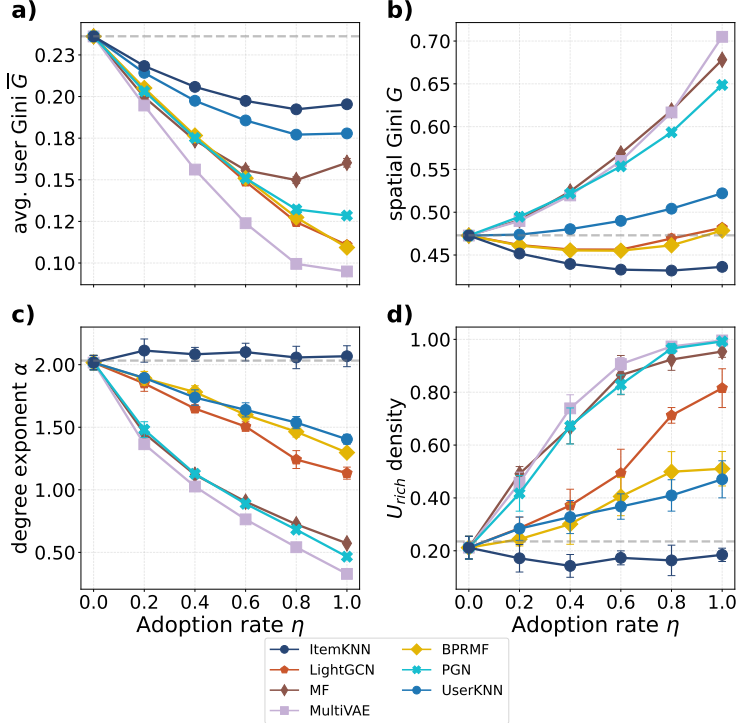


Fig. D1: Effects of recommender system adoption η considering also PGN.

Appendix D PGN

Even when using a recommender such as PGN, which incorporates spatial features, the overall dynamics remain largely unchanged. As shown in Figure D1, the algorithm exhibits patterns similar to those observed with “extreme” recommenders like MF and MultiVAE. At the spatial level, PGN leads to a notable reduction in user-level Gini index, accompanied by a significant increase in spatial Gini, indicating growing spatial inequality. At the social level, we observe a substantial decrease in the degree exponent α of the co-location network, suggesting a shift toward more homogenous connectivity, alongside the emergence of a denser rich-club structure.